

# Decadal variations in the Southern Ocean carbon sink in MPI-ESM 100 ensemble simulations

Aaron Spring,<sup>1</sup> Hongmei Li,<sup>1</sup> Tatiana Ilyina<sup>1</sup>

<sup>1</sup>Max Planck Institute for Meteorology, Bundesstraße 53, 20146 Hamburg, Germany

May 24, 2017



Max-Planck-Institut  
für Meteorologie

# Southern Ocean carbon sink

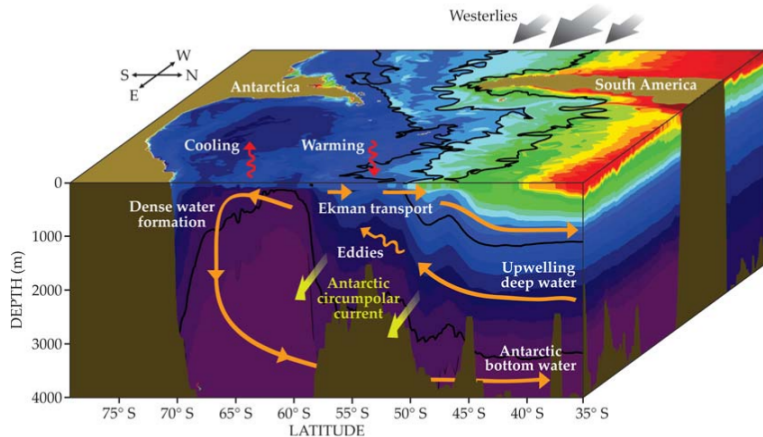


**Figure:** Dynamics of the Southern Ocean  
[Morrison et al., 2015]

Ocean-side changes in CO<sub>2</sub> flux:

- ▶ thermal
- ▶ circulation
- ▶ biology

$$\text{CO}_2\text{flux} = k_w \cdot \underbrace{(p\text{CO}_{2,\text{ocean}} - p\text{CO}_{2,\text{atm}})}_{\Delta p\text{CO}_2}$$



Recent observations suggest pronounced decadal variations in the Southern Ocean carbon sink.

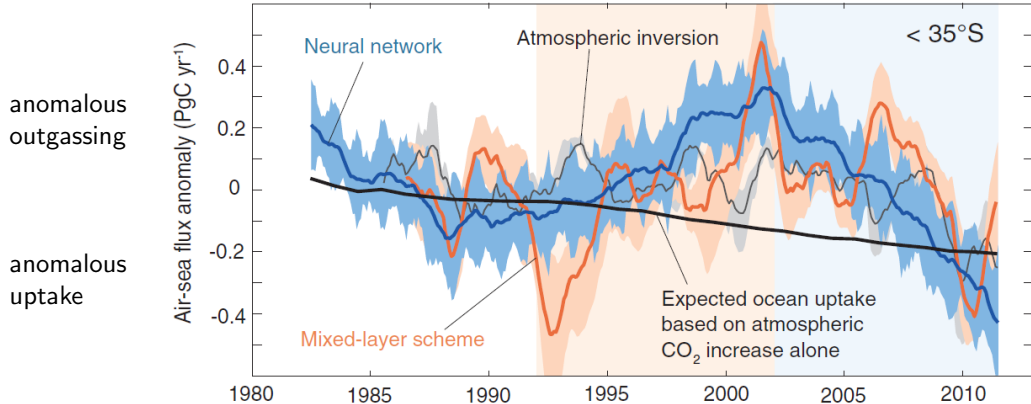


**Figure:** Evolution of the Southern Ocean carbon sink anomaly south of  $35^{\circ}\text{S}$ . Negative  $\text{CO}_2$  flux values indicate anomalous ocean uptake with respect to the 1980s mean [Landschützer et al., 2015].



However, due to the sparse spatial and temporal coverage, it is challenging to discern the dynamics of internally varying processes.

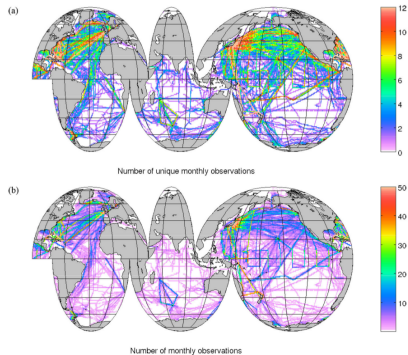


**Figure:** The number of (a) months of the year and (b) total months with surface water pCO<sub>2</sub> from 1970 to 2011 in SOCATv2  
[Bakker et al., 2014]



However, due to the sparse spatial and temporal coverage, it is challenging to discern the dynamics of internally varying processes.

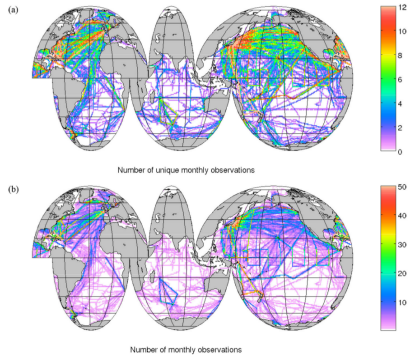


**Figure:** The number of (a) months of the year and (b) total months with surface water  $p\text{CO}_2$  from 1970 to 2011 in SOCATv2 [Bakker et al., 2014]

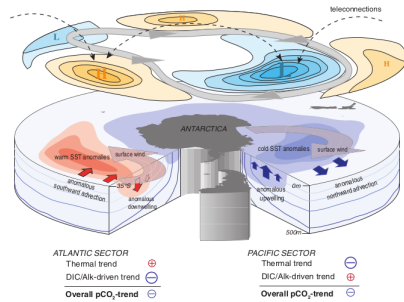


**Figure:** Schematic of the processes governing the changes in  $\Delta p\text{CO}_2$  trends in the Southern Ocean since 2001 [Landschützer et al., 2015]

Earth system models, while being a useful tool to analyze processes that contribute to variability, do not always capture this variability.

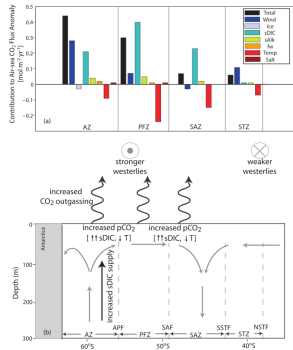


**Figure:** Contribution to air-sea  $\text{CO}_2$  flux anomaly and schematic illustration of the upper ocean response to a positive phase of the SAM [Lovenduski et al., 2007]

Earth system models, while being a useful tool to analyze processes that contribute to variability, do not always capture this variability.

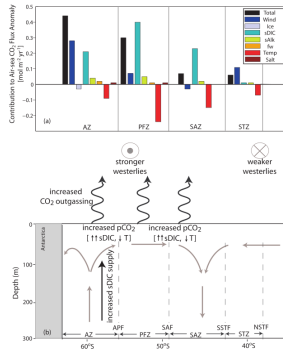


**Figure:** Contribution to air-sea  $\text{CO}_2$  flux anomaly and schematic illustration of the upper ocean response to a positive phase of the SAM [Lovenduski et al., 2007]

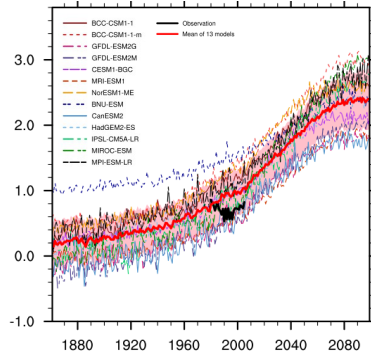


**Figure:** Historical and projected total air-sea  $\text{CO}_2$  fluxes in the Southern Ocean simulated by 13 CMIP5 models [Wang et al., 2016]

By analyzing a large ensemble of 100 historical simulations based on Max Planck Institute Earth System Model (MPI-ESM) with slightly different initial conditions but identical forcing, we assess modeled internal variability of the Southern Ocean carbon sink.

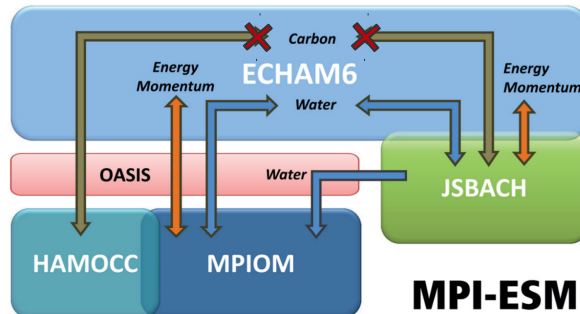


**Figure:** Schematic view of MPI-ESM1.1 with prescribed atmospheric  $\text{pCO}_2$  [Giorgetta et al., 2013]



By analyzing a large ensemble of 100 historical simulations based on Max Planck Institute Earth System Model (MPI-ESM) with slightly different initial conditions but identical forcing, we assess modeled internal variability of the Southern Ocean carbon sink.

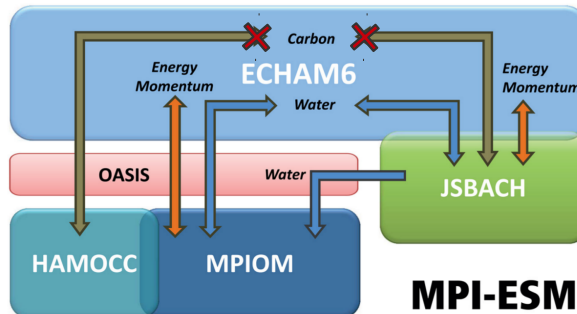


**Figure:** Schematic view of MPI-ESM1.1 with prescribed atmospheric  $\text{pCO}_2$  [Giorgetta et al., 2013]

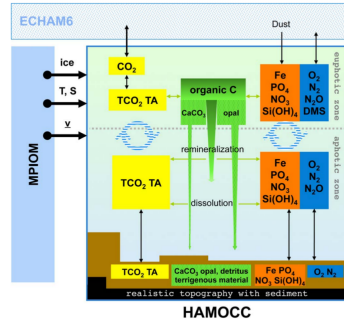


**Figure:** Schematic view of HAMOCC [Ilyina et al., 2013]

## Scientific questions

1. How large is the modeled decadal internal variability in the Southern Ocean carbon sink?



## Scientific questions

1. How large is the modeled decadal internal variability in the Southern Ocean carbon sink?
2. Do we find similar trends to those observed in the 1990s and 2000s in this large ensemble?



## Scientific questions

1. How large is the modeled decadal internal variability in the Southern Ocean carbon sink?
2. Do we find similar trends to those observed in the 1990s and 2000s in this large ensemble?
3. Which processes drive decadal internal variability in this large ensemble?



# What is internal variability?

$$\text{signal} = \underbrace{\text{forced signal}}_{\text{ensemble mean}} + \underbrace{\text{internal variability}}_{\text{residual}}$$

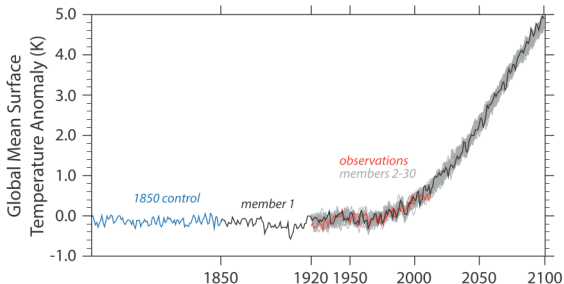


**Figure:** Global surface temperature anomaly [Kay et al., 2015]



# What is internal variability?

$$\text{signal} = \underbrace{\text{forced signal}}_{\text{ensemble mean}} + \underbrace{\text{internal variability}}_{\text{residual}}$$

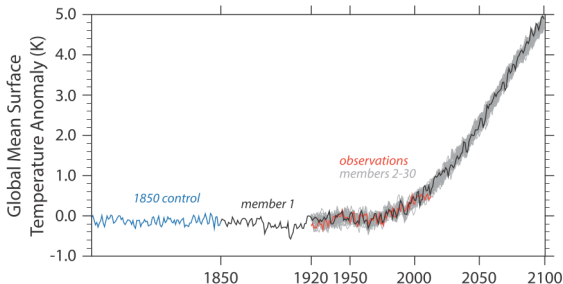


**Figure:** Global surface temperature anomaly [Kay et al., 2015]

I define decadal internal variability  $\sigma_{DIV}$  as the standard deviation of differences of the annual mean state after a decade over all  $N$  ensemble members and  $M$  decades.

$$\sigma_{DIV}(X) = \sqrt{\frac{1}{MN} \sum_{n=\text{ens}}^N \sum_{m=\text{yr}}^M (\chi_{m,n} - \bar{\chi}_{m,n})^2} \quad \chi_{m,n} = X_{\text{decade}_{\text{end}},n} - X_{\text{decade}_{\text{start}},n}$$



The modeled internal decadal variability  $\sigma_{DIV}$  is 0.18 PgC/yr.

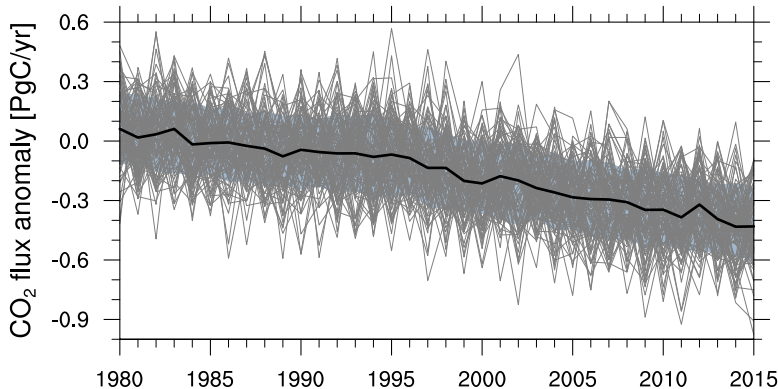


**Figure:** Temporal evolution of the Southern Ocean air-sea CO<sub>2</sub> flux anomaly south of 35°S. Grey lines show the 100 ensemble members, the black line the ensemble mean, the blue shading is the ensemble decadal internal variability  $\sigma_{DIV}$ ; negative values indicate anomalous carbon uptake.



We find positive and negative decadal CO<sub>2</sub> flux trends similar to observations in the 1990s and 2000s.

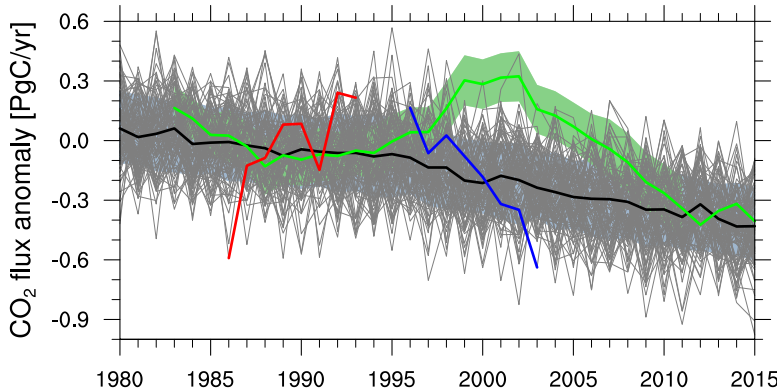


**Figure:** Temporal evolution of the Southern Ocean air-sea CO<sub>2</sub> flux anomaly south of 35°S. The red line shows a positive CO<sub>2</sub> flux trend, the blue line shows a negative CO<sub>2</sub> flux trend, the green line represents the SOM-FFN observation-based estimate [Landschützer et al., 2015].



The decadal internal variability  $\sigma_{DIV}$  is largest at 50-60°S.

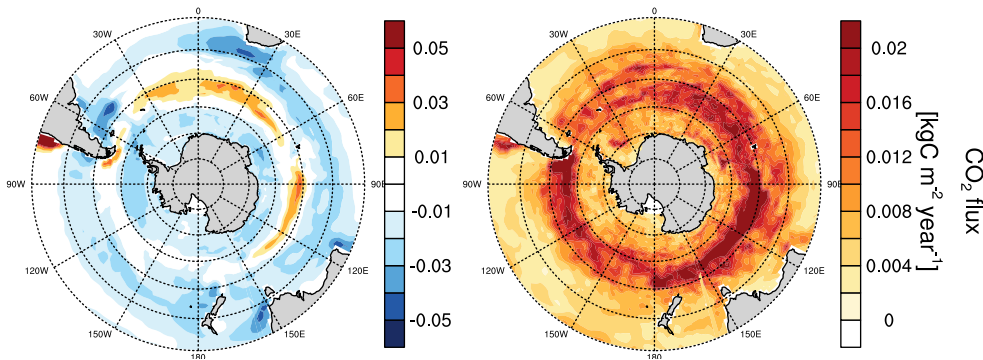


**Figure:** Spatial distribution of the climatology and decadal internal variability  $\sigma_{DIV}$  from 1980-2004 of the Southern Ocean air-sea CO<sub>2</sub> flux: MPI-ESM LE ensemble mean as forced signal and ensemble decadal standard deviation as decadal internal variability  $\sigma_{DIV}$ ; negative values indicate ocean uptake.



We find westerly winds as the main driver of internal variability.

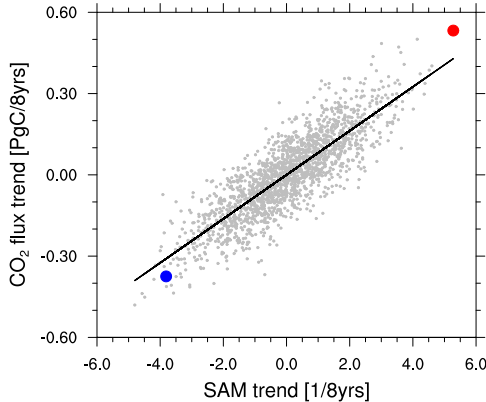


**Figure:** Linear trends in the Southern Annular Mode (SAM) as indicator of wind strength vs. CO<sub>2</sub> flux at 50-60°S; each data point represents 8-year trends of a single realization normalized for the ensemble mean trend between 1980 and 2005; the blue dot is the most negative monotonic CO<sub>2</sub> flux trend; the red dot is positive monotonic CO<sub>2</sub> flux trend.



# Southern Ocean Review

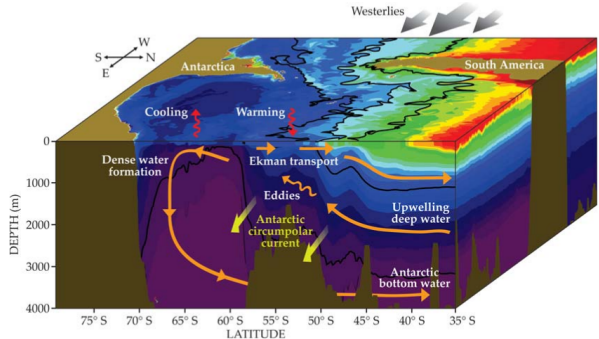


**Figure:** Dynamics of the Southern Ocean  
[Morrison et al., 2015]

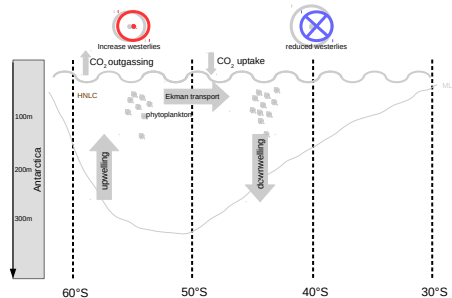


**Figure:** Schematic illustration of the Southern Ocean under the context of increasing and southward shifted westerly winds. Red color-coding means increase, blue decrease.

Enhanced and southward shifted westerly winds induce positive CO<sub>2</sub> flux trends. What's the response in thermal pCO<sub>2</sub>, biology and ocean circulation?

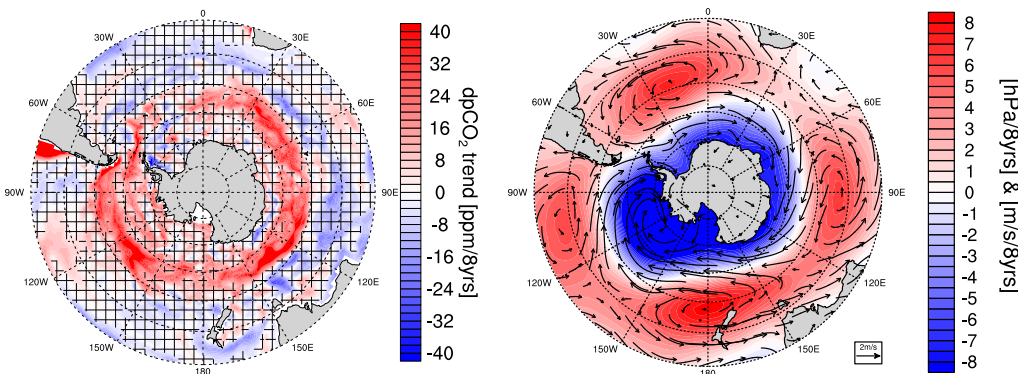


**Figure:** Linear trends in  $\Delta p\text{CO}_2$  (left) and sea-level pressure & winds (right) for the case of the most positive monotonic 8-year CO<sub>2</sub> flux trend; hatched areas indicate where trends are outside the 5%



# The non-thermal trend dominates over the thermal.

[Takahashi et al., 2002]:

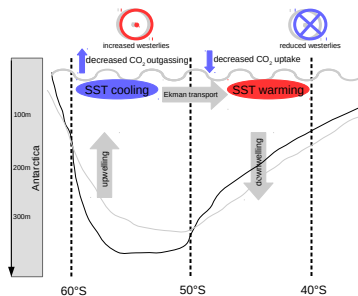


**Figure:** Schematic illustration of the thermal CO<sub>2</sub> flux response for increasing westerly winds

$$pCO_{2,\text{thermal}} = \overline{pCO_2} \cdot \exp [0.0423^{\circ}C^{-1} (T - \bar{T})]$$
$$pCO_{2,\text{non-thermal}} = pCO_2 \cdot \exp [0.0423^{\circ}C^{-1} (\bar{T} - T)]$$

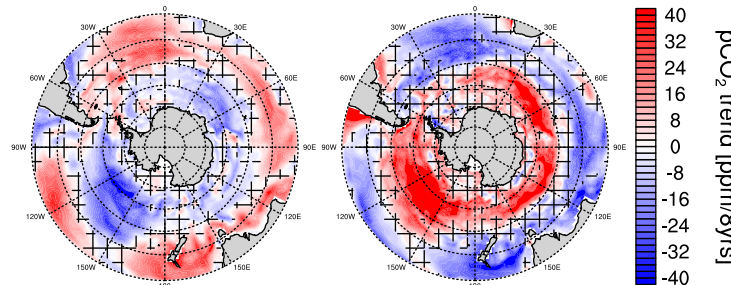


**Figure:** Linear trends in pCO<sub>2,thermal</sub> (left) and  $\Delta pCO_{2,\text{non-thermal}}$  (right) for the case of the most positive monotonic 8-year CO<sub>2</sub> flux trend; hatched areas indicate where trends are outside the 5% significance level



# Upper-ocean overturning circulation is enhanced.

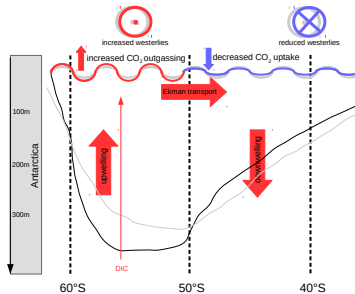


**Figure:** Schematic illustration of the circulation CO<sub>2</sub> flux response for increasing westerly winds

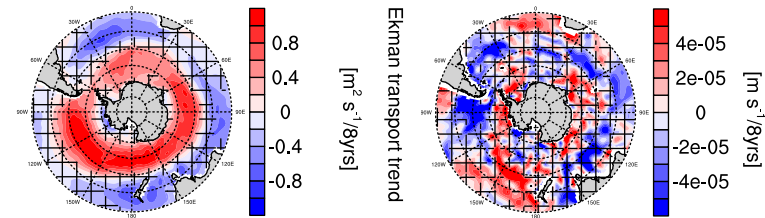


**Figure:** Linear trends in Ekman transport and Ekman pumping in the case of the most positive 8-year CO<sub>2</sub> flux trend; hatched areas indicate where trends are outside the 5% significance level

# Upper-ocean overturning circulation is enhanced and drives outgassing.

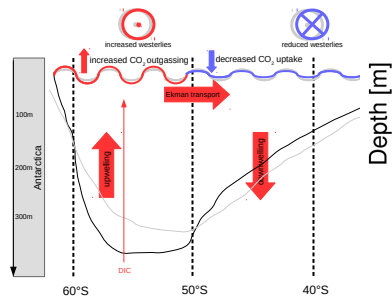


**Figure:** Schematic illustration of the circulation CO<sub>2</sub> flux response for increasing westerly winds

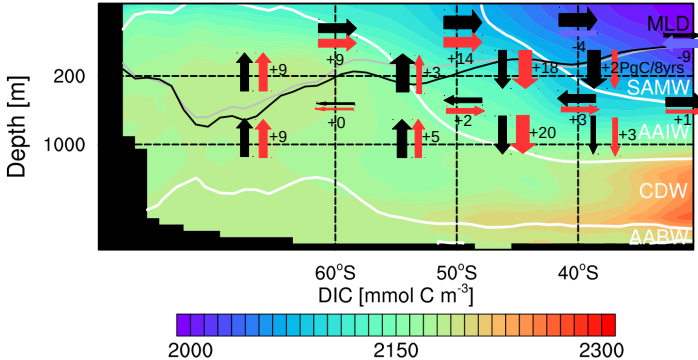


**Figure:** Zonally averaged upper-ocean overturning circulation in the case of the most positive 8-year CO<sub>2</sub> flux trend; similar [DeVries et al., 2017]

Primary production trends oppose CO<sub>2</sub> flux trends, but not caused by changes in nutrients.

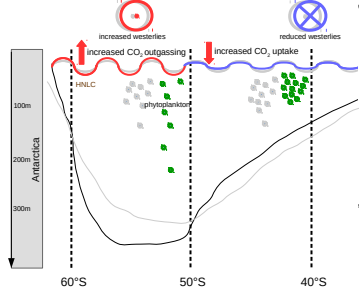


**Figure:** Schematic illustration of the biological CO<sub>2</sub> flux response for increasing westerly winds

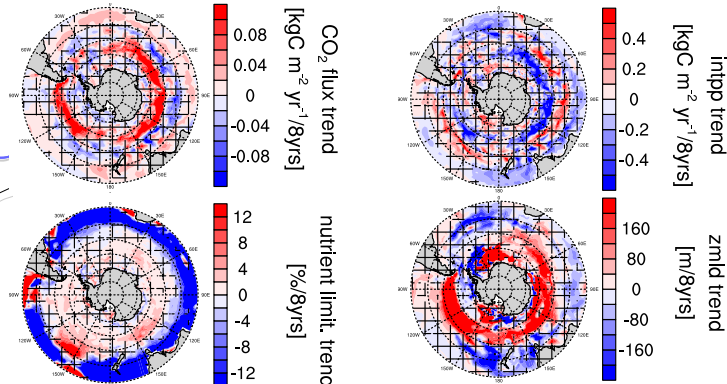


**Figure:** Southern Ocean austral summer trends over 8 years: CO<sub>2</sub> flux (top left), vertically integrated primary production (top right), surface nutrient limitation (bottom left) and mixed layer depth (bottom right); hatched areas indicate where trends are outside the 5% significance level

Light & temperature limitation causes the decline in primary production at 50-60°S. Phytoplankton gets mixed deeper into the ocean.

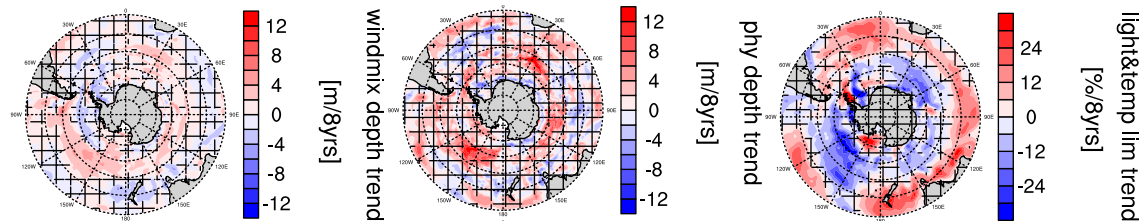


**Figure:** Trends in of average depth of vertical diffusivity due to wind (left), phytoplankton average depth (middle) and surface light & temperature limitation factor; hatched areas indicate where trends are outside the 5% significance level

Previous studies show increasing primary production for increasing winds. Increased upwelling brings more nutrients, but this has no effect on biology in HAMOCC. However, biology signal much smaller than circulation.

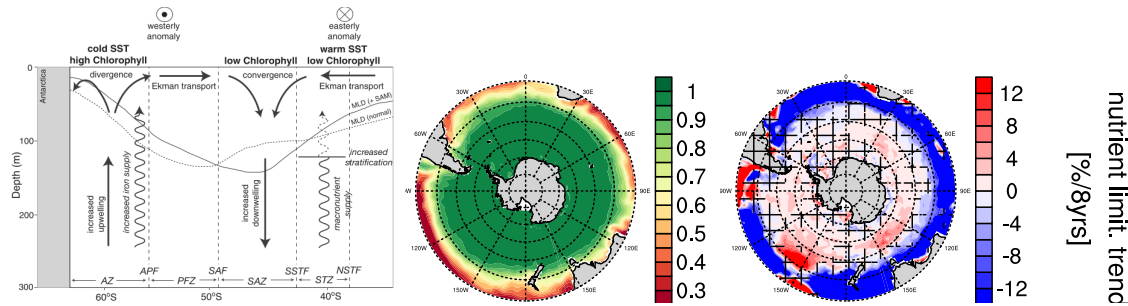


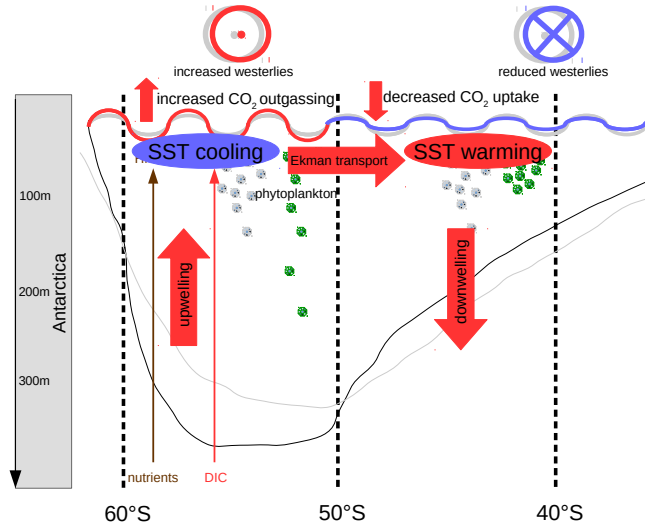
**Figure:** (left) Schematic view of the upper ocean response to a positive SAM phase [Lovenduski and Gruber, 2005]; (right) surface nutrient limitation function summer mean and trend

related papers: [Lovenduski et al., 2008] [Wang and Moore, 2012] [Hauck et al., 2013]

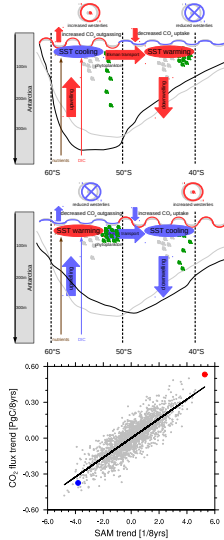


# Intensified winds reduce the overall Southern Ocean carbon sink.

thermal	-
circulation	+
biology	+
<b>total</b>	<b>+</b>

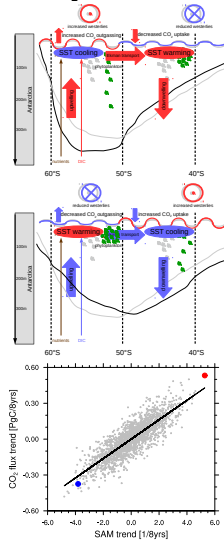


# Summary



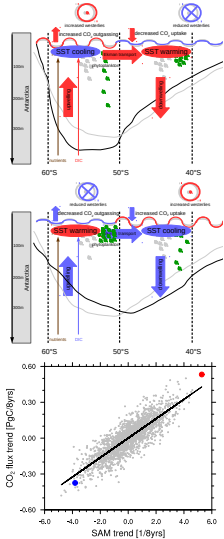
- Modeled decadal internal variability  $\sigma_{DIV} \approx 0.18 \text{ PgC/yr}$  and is largest at 50-60°S

# Summary



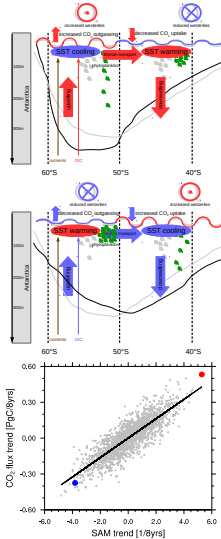
- Modeled decadal internal variability  $\sigma_{DIV} \approx 0.18 \text{ PgC/yr}$  and is largest at 50-60°S
- MPI-ESM Large Ensemble captures multi-year positive and negative trends as suggested by observations

# Summary



- Modeled decadal internal variability  $\sigma_{DIV} \approx 0.18 \text{ PgC/yr}$  and is largest at 50-60°S
- MPI-ESM Large Ensemble captures multi-year positive and negative trends as suggested by observations
- Trends reverse for decreasing winds

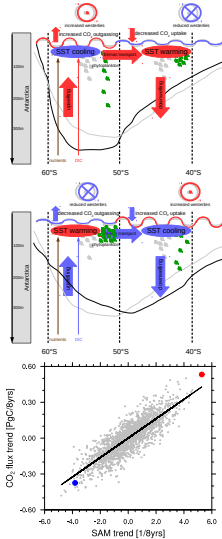
# Summary



- Modeled decadal internal variability  $\sigma_{DIV} \approx 0.18 \text{ PgC/yr}$  and is largest at 50-60°S
- MPI-ESM Large Ensemble captures multi-year positive and negative trends as suggested by observations
- Trends reverse for decreasing winds
- We find two wind-driven regimes of the Southern Ocean carbon sink: Enhanced winds...

Overall, this weakens the carbon sink and vice versa strengthens for weaker winds.

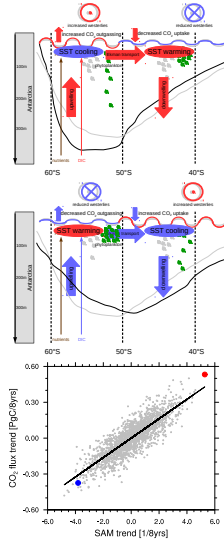
# Summary



- Modeled decadal internal variability  $\sigma_{DIV} \approx 0.18 \text{ PgC/yr}$  and is largest at 50-60°S
- MPI-ESM Large Ensemble captures multi-year positive and negative trends as suggested by observations
- Trends reverse for decreasing winds
- We find two wind-driven regimes of the Southern Ocean carbon sink: Enhanced winds...
  - increase thermal CO<sub>2</sub> uptake

Overall, this weakens the carbon sink and vice versa strengthens for weaker winds.

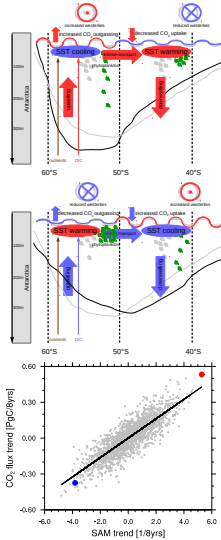
# Summary



- Modeled decadal internal variability  $\sigma_{DIV} \approx 0.18 \text{ PgC/yr}$  and is largest at 50-60°S
- MPI-ESM Large Ensemble captures multi-year positive and negative trends as suggested by observations
- Trends reverse for decreasing winds
- We find two wind-driven regimes of the Southern Ocean carbon sink: Enhanced winds...
  - increase thermal CO<sub>2</sub> uptake
  - increase upwelling

Overall, this weakens the carbon sink and vice versa strengthens for weaker winds.

# Summary



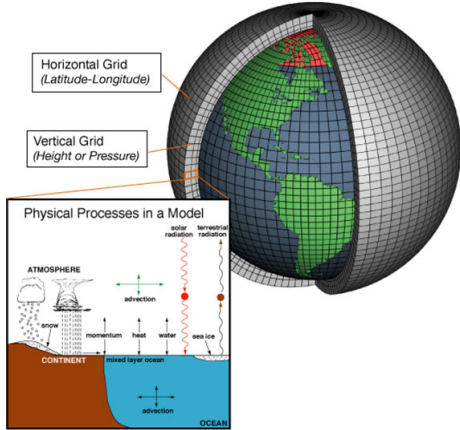
- Modeled decadal internal variability  $\sigma_{DIV} \approx 0.18 \text{ PgC/yr}$  and is largest at 50-60°S
- MPI-ESM Large Ensemble captures multi-year positive and negative trends as suggested by observations
- Trends reverse for decreasing winds
- We find two wind-driven regimes of the Southern Ocean carbon sink: Enhanced winds...
  - increase thermal CO<sub>2</sub> uptake
  - increase upwelling
  - decrease primary production

Overall, this weakens the carbon sink and vice versa strengthens for weaker winds.

# Appendix



# Earth-system-modeling

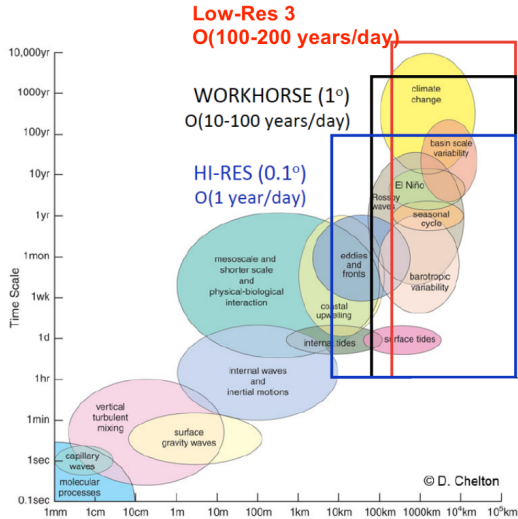


HAMOCC Visualisation:

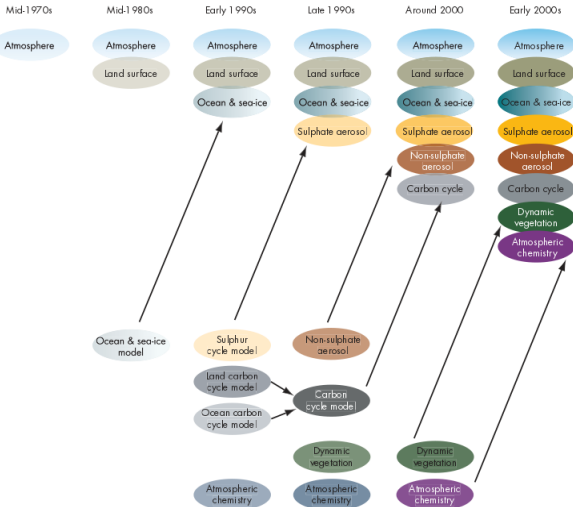
<https://www.dkrz.de/about/media/galerie/Vis/esm/hamocc>



# Earth-system-model scales



# Earth-system-model processes



# CO<sub>2</sub> flux Southern Ocean Trendmap

CO<sub>2</sub>flux trends heatmap in MPI-ESM Large Ensemble

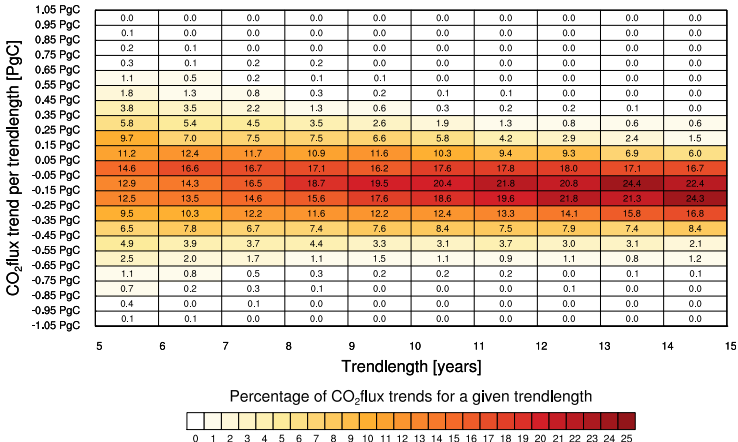
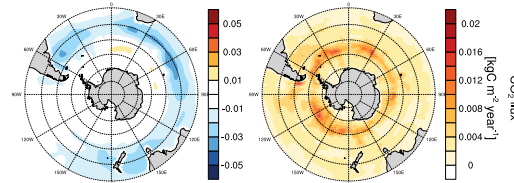
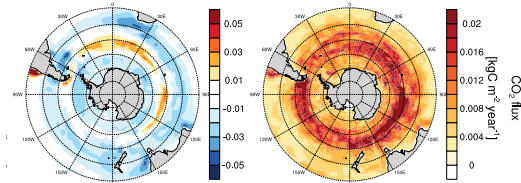


Figure: Southern Ocean carbon sink trends per trendlength



# Model Evaluation - CO<sub>2</sub> flux



**Figure:** Spatial distribution of the climatology (a,c) and decadal internal variability  $\sigma_{DIV}$  (b,d) from 1980-2004 of the Southern Ocean air-sea CO<sub>2</sub> flux: MPI-ESM LE ensemble mean as forced signal (a), ensemble decadal standard deviation as decadal internal variability  $\sigma_{DIV}$  (b), SOM-FFN climatology 1982-2004 (c), SOM-FFN decadal variability  $\sigma_{DIV}$  (d); negative values indicate ocean uptake.

# Model Evaluation - Winds

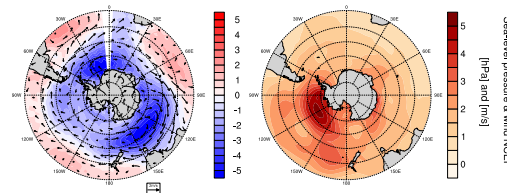
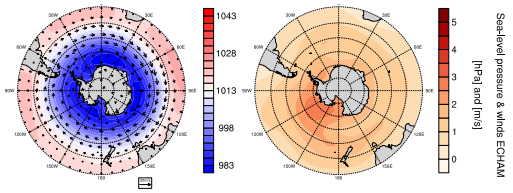


**Figure:** Spatial distribution of the Southern Ocean sea-level pressure and winds: ensemble mean climatology from 1980 to 2004 (a) as forced signal and ensemble decadal standard deviation (b) as decadal internal variability  $\sigma_{DIV}$ ; and the difference between MPI-ESM and reanalysis data from NCEP climatology (c), and decadal internal variability  $\sigma_{DIV}$  from NCEP climatology (d).

# Model Evaluation - Nutrients

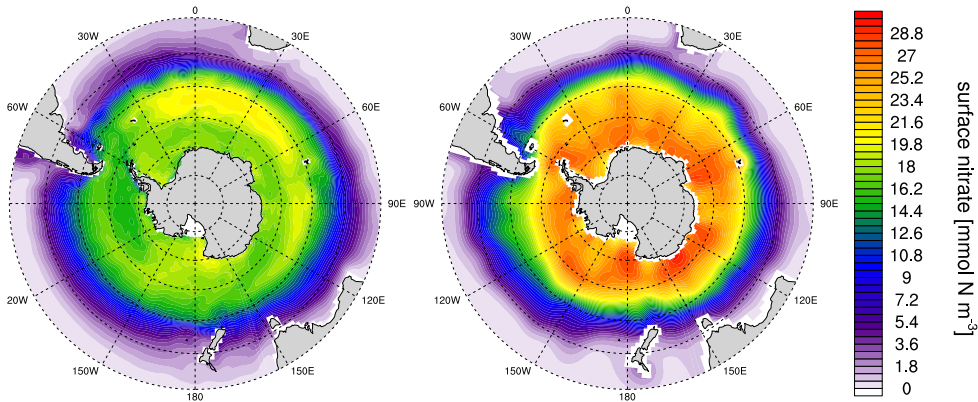


**Figure:** Spatial distribution of the climatology of surface nitrate (left) compared with WOA data [Garcia et al., 2013] (right)



# Model Evaluation - SST

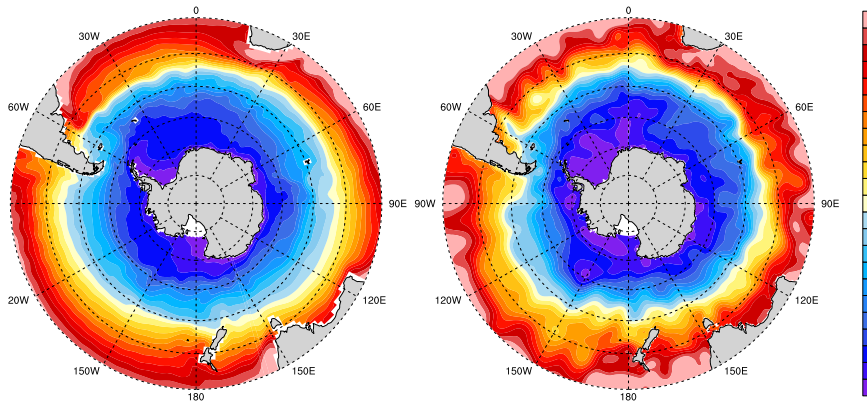


**Figure:** Spatial distribution of the ensemble mean climatology (1980-2004) of the sea-surface temperature (SST) (left) compared with xyz



# References I

D. C. E. Bakker, B. Pfeil, K. Smith, S. Hankin, A. Olsen, S. R. Alin, C. Cosca, S. Harasawa, A. Kozyr, Y. Nojiri, K. M. O'Brien, U. Schuster, M. Telszewski, B. Tilbrook, C. Wada, J. Akl, L. Barbero, N. R. Bates, J. Boutin, Y. Bozec, W.-J. Cai, R. D. Castle, F. P. Chavez, L. Chen, M. Chierici, K. Currie, H. J. W. de Baar, W. Evans, R. A. Feely, A. Fransson, Z. Gao, B. Hales, N. J. Hardman-Mountford, M. Hoppema, W.-J. Huang, C. W. Hunt, B. Huss, T. Ichikawa, T. Johannessen, E. M. Jones, S. D. Jones, S. Jutterstrm, V. Kitidis, A. Krtzinger, P. Landschtzer, S. K. Lauvset, N. Lefèvre, A. B. Manke, J. T. Mathis, L. Merlivat, N. Metzl, A. Murata, T. Newberger, A. M. Omar, T. Ono, G.-H. Park, K. Paterson, D. Pierrot, A. F. Ríos, C. L. Sabine, S. Saito, J. Salisbury, V. V. S. S. Sarma, R. Schlitzer, R. Sieger, I. Skjelvan, T. Steinhoff, K. F. Sullivan, H. Sun, A. J. Sutton, T. Suzuki, C. Sweeney, T. Takahashi, J. Tjiputra, N. Tsurushima, S. M. A. C. van Heuven, D. Vandemark, P. Vlahos, D. W. R. Wallace, R. Wanninkhof, and A. J. Watson. An update to the surface ocean CO<sub>2</sub> atlas (SOCAT version 2). *Earth*



## References II

- System Science Data*, 6(1):69–90, mar 2014. doi: 10.5194/essd-6-69-2014. URL <https://doi.org/10.5194%2Fessd-6-69-2014>.
- T. DeVries, M. Holzer, and F. Primeau. Recent increase in oceanic carbon uptake driven by weaker upper-ocean overturning. *Nature*, 542(7640):215–218, feb 2017. doi: 10.1038/nature21068. URL <https://doi.org/10.1038%2Fnature21068>.
- H. E. Garcia, R. A. Locarnini, T. P. Boyer, J. I. Antonov, O. Baranova, M. Zweng, J. Reagan, and D. Johnson. *World Ocean Atlas 2013, Volume 4: Dissolved Inorganic Nutrients (phosphate, nitrate, silicate)*, volume 76 of 25. NOAA Atlas NESDIS, 2013. URL <https://www.nodc.noaa.gov/OC5/woa13/pubwoa13.html>.



## References III

- M. A. Giorgetta, J. Jungclaus, C. H. Reick, S. Legutke, J. Bader, M. Böttinger, V. Brovkin, T. Crueger, M. Esch, K. Fieg, K. Glushak, V. Gayler, H. Haak, H.-D. Hollweg, T. Illyina, S. Kinne, L. Kornblueh, D. Matei, T. Mauritzen, U. Mikolajewicz, W. Mueller, D. Notz, F. Pithan, T. Raddatz, S. Rast, R. Redler, E. Roeckner, H. Schmidt, R. Schnur, J. Segschneider, K. D. Six, M. Stockhouse, C. Timmreck, J. Wegner, H. Widmann, K.-H. Wieners, M. Claussen, J. Marotzke, and B. Stevens. Climate and carbon cycle changes from 1850 to 2100 in mpi-esm simulations for the coupled model intercomparison project phase 5. *Journal of Advances in Modeling Earth Systems*, 5(3):572–597, 2013. ISSN 1942-2466. doi: 10.1002/jame.20038. URL <http://dx.doi.org/10.1002/jame.20038>.
- J. Hauck, C. Völker, T. Wang, M. Hoppema, M. Losch, and D. A. Wolf-Gladrow. Seasonally different carbon flux changes in the southern ocean in response to the southern annular mode. *Global Biogeochemical Cycles*, 27(4):1236–1245, dec 2013. doi: 10.1002/2013gb004600. URL <http://dx.doi.org/10.1002/2013GB004600>.



## References IV

- T. Illyina, K. D. Six, J. Segschneider, E. Maier-Reimer, H. Li, and I. Núñez-Riboni. Global ocean biogeochemistry model hamocc: Model architecture and performance as component of the mpi-earth system model in different cmip5 experimental realizations. *Journal of Advances in Modeling Earth Systems*, 5(2):287–315, 2013. ISSN 1942-2466. doi: 10.1029/2012MS000178. URL <http://dx.doi.org/10.1029/2012MS000178>.
- J. E. Kay, C. Deser, A. Phillips, A. Mai, C. Hannay, G. Strand, J. M. Arblaster, S. C. Bates, G. Danabasoglu, J. Edwards, M. Holland, P. Kushner, J.-F. Lamarque, D. Lawrence, K. Lindsay, A. Middleton, E. Munoz, R. Neale, K. Oleson, L. Polvani, and M. Vertenstein. The community earth system model (CESM) large ensemble project: A community resource for studying climate change in the presence of internal climate variability. *Bull. Amer. Meteor. Soc.*, 96(8):1333–1349, aug 2015. doi: 10.1175/bams-d-13-00255.1. URL <http://dx.doi.org/10.1175/BAMS-D-13-00255.1>.



## References V

- P. Landschützer, N. Gruber, F. A. Haumann, C. Rödenbeck, D. C. E. Bakker, S. van Heuven, M. Hoppema, N. Metzl, C. Sweeney, T. Takahashi, B. Tilbrook, and R. Wanninkhof. The reinvigoration of the southern ocean carbon sink. *Science*, 349(6253):1221–1224, 2015. ISSN 0036-8075. doi: 10.1126/science.aab2620. URL <http://science.scienmag.org/content/349/6253/1221>.
- N. S. Lovenduski and N. Gruber. Impact of the southern annular mode on southern ocean circulation and biology. *Geophys. Res. Lett.*, 32(L11603), 2005. doi: 10.1029/2005GL022727. URL <http://onlinelibrary.wiley.com/doi/10.1029/2005GL022727/pdf>.
- N. S. Lovenduski, N. Gruber, S. C. Doney, and I. D. Lima. Enhanced  $\text{CO}_2$  outgassing in the southern ocean from a positive phase of the southern annular mode. *Global Biogeochemical Cycles*, 21(2), 2007. ISSN 1944-9224. doi: 10.1029/2006GB002900. URL <http://dx.doi.org/10.1029/2006GB002900>. GB2026.



## References VI

- N. S. Lovenduski, N. Gruber, and S. C. Doney. Toward a mechanistic understanding of the decadal trends in the southern ocean carbon sink. *Global Biogeochem. Cycles*, 22, 2008. doi: 10.1029/2007GB003139.
- A. Morrison, T. Frölicher, and J. Sarmiento. Upwelling in the southern ocean. *Physics Today*, 2015. doi: 10.1063/PT.3.2654. URL <http://dx.doi.org/10.1063/PT.3.2654>.
- T. Takahashi, S. C. Sutherland, C. Sweeney, A. Poisson, N. Metzl, B. Tilbrook, N. Bates, R. Wanninkhof, R. A. Feely, C. Sabine, J. Olafsson, and Y. Nojiri. Global seaair  $\text{CO}_2$  flux based on climatological surface ocean and pco and seasonal biological and temperature effects. *Deep-Sea Research II*, 2002.
- L. Wang, J. Huang, Y. Luo, and Z. Zhao. Narrowing the spread in CMIP5 model projections of air-sea  $\text{CO}_2$  fluxes. *Scientific Reports*, 6:37548, nov 2016. doi: 10.1038/srep37548. URL <https://doi.org/10.1038%2Fsrep37548>.



## References VII

S. Wang and J. K. Moore. Variability of primary production and air-sea CO<sub>2</sub> flux in the Southern Ocean. *Global Biogeochemical Cycles*, 26(1):n/an/a, 2012. ISSN 1944-9224. doi: 10.1029/2010GB003981. URL  
<http://dx.doi.org/10.1029/2010GB003981>. GB1008.

